DRAG AND DRAG PARTITION ON ROUGH SURFACES

M. R. RAUPACH

CSIRO Centre for Environmental Mechanics, GPO Box 821, Canberra, ACT 2601, Australia

(Received in final form 6 February, 1992)

Abstract. An analytic treatment of drag and drag partition on rough surfaces is given. The aims are to provide simple predictive expressions for practical applications, and to rationalize existing laboratory and atmospheric data into a single framework. Using dimensional analysis and two physical hypotheses, theoretical predictions are developed for total stress (described by the square root of the canopy drag coefficient), stress partition (described by the ratio τ_S/τ of the stress τ_S on the underlying ground surface to total stress τ), zero-plane displacement and roughness length. The stress partition prediction is the simple equation $\tau_S/\tau = 1/(1 + \beta\lambda)$, where $\beta = C_R/C_S$ is the ratio of element and surface drag coefficients. This prediction agrees very well with data and is free of adjustable constants. Other predictions also agree well with a range of laboratory and atmospheric data.

1. Introduction

When one considers the drag exerted on a rough surface by deep, fully developed, turbulent boundary-layer flow, one immediately confronts two problems which are simple to state but, as yet, remain unsolved in general. Firstly, given a particular roughness geometry, what is the total surface drag or drag coefficient? Secondly, what is the partition of drag between the roughness elements and the underlying substrate surface? This paper attempts a fairly general, approximate treatment of both questions, independent of the numerous practical applications. The specific practical issue which motivated this work – how roughness elements ameliorate wind erosion – is treated in another paper (Raupach *et al.*, 1992).

The first question – that of total drag – has been the subject of extensive experimental studies in both laboratory and atmospheric layers: see, for example, reviews by Yaglom (1979) and Raupach *et al.* (1991). The drag (the total shear stress on the rough surface, or the downward flux density of streamwise momentum to the surface) may be specified with a drag coefficient

$$C_D(z) = \tau/\rho U(z)^2 = u_*^2/U(z)^2\,, \tag{1}$$

where $U(z)$ is mean velocity at height z, τ total surface shear stress, ρ air density and u_* the friction velocity, defined by $\tau = \rho u_*^2$. (The coordinates x, y, z lie in the streamwise, lateral and vertical directions, respectively, with $z = 0$ the underlying substrate surface). An alternative specification of the drag is through the roughness length z_0 in the logarithmic law for the mean velocity profile in the inertial sublayer

Boundary-Layer Meteorology **60**: 375–395, 1992.

or logarithmic layer,

$$\frac{U(z)}{u_*} = \frac{1}{\kappa}\ln\left(\frac{z-d}{z_0}\right), \tag{2}$$

where κ (≈ 0.4) is the von Karman constant and d is the zero-plane displacement or height of aerodynamic origin. Unlike C_D (which is z-dependent), z_0 depends only on geometric properties of the surface, such as roughness element height h, breadth b and spacing D, provided the flow is dynamically fully rough. An approximate condition for fully rough flow is $hu_*/\nu > 55$, where ν is the kinematic viscosity (Bandyopadhyay, 1987); if this condition is not met, then z_0 also depends on ν. This work is restricted to the fully rough case.

The extensive measurements available on rough-surface drag have been summarized in several surveys; see the reviews cited above. One way of summarizing the relationship between drag and surface structure is to plot the ratio z_0/h against the roughness density (or frontal area per unit ground area)

$$\lambda = bh/D^2 = nbh/S\,, \tag{3}$$

where n roughness elements occupy ground area S. Data for both laboratory and atmospheric roughness show that z_0/h increases roughly linearly with λ for $0 < \lambda < \lambda_{\max}$, where $\lambda_{\max}$ is of order 0.1 to 0.3, and decreases with further increase in λ. The maximum z_0/h value (of order 0.1 to 0.15) and the precise form of the function $[z_0/h](\lambda)$ both depend on the geometry of the roughness elements.

In contrast with measurements, there have been few attempts to formulate general theories for rough-surface drag. Lettau (1969) proposed, and Wooding *et al.* (1973) formally justified, a linear relationship between z_0/h and λ at low roughness densities ($\lambda \ll \lambda_{\max}$). Shaw and Pereira (1982) used a one-dimensional (vertical) second-order closure model of transfer in a vegetation canopy to investigate the variation of z_0/h and d/h with λ, finding behaviour approximately in agreement with the rather scattered available data for vegetation (Raupach *et al.*, 1991). However, it is unlikely that a one-dimensional model can describe satisfactorily the highly three-dimensional flow among sparse roughness elements ($\lambda < \lambda_{\max}$).

The second question posed at the outset, that of drag partition, has been far less intensively studied than that of total drag. The total stress τ can be split into a stress τ_R on the roughness elements and a stress τ_S on the underlying surface:

$$\tau = \rho u_*^2 = \tau_R + \tau_S\,. \tag{4}$$

The partition problem is to determine the ratio τ_S/τ (or $\tau_R/\tau = 1 - \tau_S/\tau$) and its variation with λ. Note that in this paper, τ_S is defined as the area-averaged force on the substrate surface per unit ground area S. The area-averaged force per unit exposed ground area is $\tau_S' = (S/S')\tau_S = \tau_S/(1-\mu)$, where S' is the exposed

ground area and $\mu = 1 - (S'/S)$ is the basal area index (basal element area per unit ground area), analogous to the frontal area index λ defined by (3).

The most complete data on drag partition come from the wind tunnel experiments of Marshall (1971), who measured τ and τ_R separately for a variety of cylindrical and hemispheric roughness elements for λ between about 0.0002 and 0.2, thence determining τ_S by difference. The measurements of τ came both from drag plates and from momentum integral balance considerations (which agreed), while τ_R was measured by mounting individual elements on a drag balance. Theoretical approaches to the problem began with Schlichting (1936), who first wrote the partition equation (4). Wooding *et al.* (1973) suggested that $\sqrt{\tau_R/\tau}$ varies linearly with $\ln(1/\lambda) = -\ln(\lambda)$, while Arya (1975) produced a drag partition theory for two-dimensional obstacles transverse to the wind direction, with some points of similarity with the present work. A detailed comparison of these theories with the present work is given in Section 5.

This paper outlines a simple analytic treatment of drag and drag partition on rough surfaces. Without attempting to offer a complete solution to either of the problems posed at the outset, the aims are to rationalize the existing observations into a single framework, and to provide simple predictive expressions for practical applications, especially for drag partition. The approach is based on scaling and dimensional analysis. A detailed dynamical treatment of the turbulence within the roughness canopy is replaced by two heuristic assumptions, one about the scales controlling an element wake in a turbulent boundary layer, and a second about how element wakes interact.

The present paper is essentially a companion to Raupach *et al.* (1992), which considers how the threshold for wind erosion is increased by placing nonerodible roughness elements on an erodible surface. Predictions are derived from the present theory for drag partition and shown to agree well with several sets of measurements.

2. Definitions and Hypotheses

An individual roughness element (one of a population of elements on a rough surface) has a turbulent wake which exists within a deep turbulent boundary layer. Taylor (1988) pointed out that the presence of the substrate surface and the ambient boundary-layer turbulence both make the roughness-element wake more complicated than the well-known wake of an obstacle is a non-turbulent free stream. For instance, the drag on a surface-mounted roughness element does not satisfy a simple momentum integral constraint equivalent to the relationship $F = \rho UJ$ for a wake of an obstacle in a free stream (e.g., Batchelor, 1967; Lighthill, 1986) (here F is the drag force on the obstacle, U the free stream velocity and J the volume flux deficit in the wake, equal to the velocity deficit integrated over the wake cross-section). Also, a turbulent wake in a free stream is self-similar in the far field, with a cross-stream length scale proportional to $x^{1/2}$ or $x^{1/3}$ (for two-

and three-dimensional wakes, respectively), but no such simple results can be obtained unequivocally for surface-mounted roughness elements. Hence, experience with free-stream wakes is not a good guide to the wake and shelter properties of surface-mounted obstacles in turbulent boundary layers.

The starting point of the present approach is to characterize the wake of an isolated roughness element placed on the surface in terms of an *effective shelter area* A and an *effective shelter volume* V which are amenable to scale analysis. The area A, which describes the reduction of ground (substrate surface) shear stress τ_S in the element wake, is defined as the area integral of the normalized ground stress deficit:

$$A = \int\int \left(1 - \frac{\tau_S(x, y)}{\tau_{S0}}\right) \mathrm{d}x\, \mathrm{d}y\,, \tag{5}$$

where $\tau_S(x, y)$ is the actual ground stress at the point (x, y) and τ_{S0} the unsheltered ground stress in the same wind conditions, equal to $\tau_S(x, y)$ far from the isolated element. Conceptually, A is the area within which the stress on the ground must be set to zero, to produce the same integrated stress deficit as that induced by the sheltering element. Figure 1 illustrates this definition, idealizing the effective shelter area as a wedge-shaped shadow in the lee of the element. Note that the shelter area A includes the basal area of the element itself.

The effective shelter volume V describes the effect of a given roughness element upon the drag forces on other elements in its vicinity. To obtain a formal definition analogous to that for A, we consider the local force per unit volume, ϕ, on a sparse array of test obstacles: $\phi = \rho\alpha C_E(U)U^2$, with $C_E(U)$ the drag coefficient of a test obstacle and α the frontal area density (frontal area per unit volume) of the test array. (In this paper, drag coefficients are defined without a factor 1/2, in accordance with meteorological rather than aerodynamic convention). The test array must be sparse ($\alpha \to 0$) so that it senses, but does not modify, the drag properties of the flow. Then V can be defined as the volume integral of the normalized deficit in ϕ which is induced by placing a "sheltering" roughness element into the test array:

$$\begin{aligned} V &= \int\int\int \left(\frac{\phi_0 - \phi}{\phi_0}\right) \mathrm{d}z\, \mathrm{d}x\, \mathrm{d}y \\ &= \int\int\int \left(1 - \frac{C_E(U)U^2(x, y, z)}{C_E(U_0)U_0^2(z)}\right) \mathrm{d}z\, \mathrm{d}x\, \mathrm{d}y\,, \end{aligned} \tag{6}$$

where the subscript 0 denotes the undisturbed conditions far from the sheltering element. This volume is that within which the drag force on the array of test obstacles must be set to zero, to produce the same integrated force deficit as that induced by the sheltering element. This definition is also illustrated in Figure 1, again idealizing the effective shelter volume as a wedge-shaped region. As in the

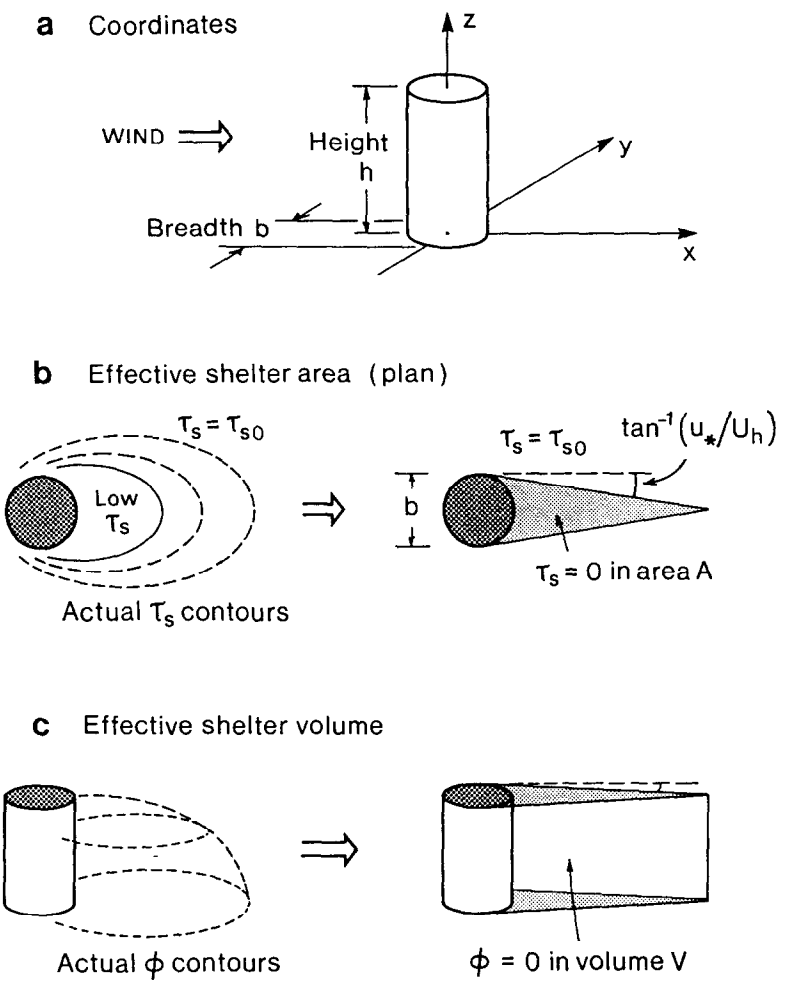

Fig. 1. Definition sketches for effective shelter area and effective shelter volume.

case of shelter area, the shelter volume V includes the volume occupied by the sheltering element itself.

Two hypotheses are now introduced, one to specify the external scales controlling the shelter area A and volume V for a single roughness element, and the second to describe interactions between roughness elements.

Hypothesis I

For an isolated roughness element of breadth b and height h in a deep turbulent boundary layer with friction velocity u_* and mean velocity U_h at height h, the

effective shelter area A and volume V scale as

$$A \sim b^2 U_h/u_*\,, \qquad V \sim b^2 h\, U_h/u_*\,, \tag{7a}$$

in the case where h is significantly greater than b, and as

$$A \sim bh\, U_h/u_*\,, \qquad V \sim bh^2\, U_h/u_*\,, \tag{7b}$$

in the case where h is significantly less than b.

A physical basis for this scaling is as follows: in the near-wake region, the wake of an isolated roughness element is bounded by strong shear layers in which the vorticity is locally high, with the vorticity vector lying approximately in the plane of the local shear layer and normal to the local mean flow direction. This vorticity advects in the streamwise direction at a velocity of order U_h, and spreads by turbulent diffusion in the cross-stream direction with a velocity of order u_*, determined by the ambient turbulence in which the shear layer exists (a different situation from a wake in a uniform free stream, which is controlled by the wake turbulence itself). Hence, the shear layers bounding the wake spread at an angle of order U_h/u_* to the streamwise direction. Finnigan *et al.* (1990) used similar arguments successfully to infer the depth of the inner layer (the region of strongly modified turbulence) for wind flow over a hill. It follows that the strongly sheltered region behind the element is roughly the shape of a tapered wedge with semi-angle of order U_h/u_*, as in Figure 1. The ground area and volume of this wedge scale according to (7a) or (7b), depending on whether the area and volume are limited by lateral growth of the shear layers (when $h \gg b$, giving (7a)) or vertical growth (when $h \ll b$, giving (7b)).

Based on (7a) and (7b), A and V can be expressed in general as

$$A = c_1'(b/h)^p\, bh\, U_h/u_*\,, \qquad V = c_2'(b/h)^p\, bh^2\, U_h/u_*\,, \tag{7c}$$

where c_1' and c_2' are $O(1)$ constants of proportionality, and the power p depends on b/h: $p = 1$ when $b/h \to 0$, and $p = 0$ when $b/h \to \infty$. It is convenient to write $c_1 = c_1'(b/h)^p$ and $c_2 = c_2'(b/h)^p$, so that (7c) takes the simpler form

$$A = c_1\, bh\, U_h/u_*\,, \qquad V = c_2\, bh^2\, U_h/u_*\,. \tag{7d}$$

Hypothesis II

When roughness elements are distributed uniformly or randomly across a surface, the combined effective shelter area or volume can be calculated by randomly superimposing individual shelter areas or volumes.

The rationale for this hypothesis is that actual velocity and ground stress deficits in the wake of an element are spread over a large region (in comparison with the area A and volume V) by the randomizing effect of the ambient turbulence in the flow. This is a plausible picture because the velocity and length scales for the ambient turbulence over a typical rough surface are both substantially larger than the corresponding scales for the wake turbulence (Raupach *et al.*, 1991).

Two further comments need to be made about Hypothesis II. First, the hypothesis not only specifies the degree of interaction between element wakes, but also asserts that the interaction is dependent only on the roughness density λ and not on the arrangement of roughness elements on the surface. Empirically, this is a reasonable approximation (Marshall, 1971). Second, there is a small contradiction in assuming that random superposition of shelter areas (or volumes) can apply to that part of the shelter area (or volume) corresponding to the basal area (or occupied volume) of a roughness element. Since two solid elements cannot occupy the same space, basal areas and occupied volumes cannot be randomly superimposed in the way that Hypothesis II suggests. Rather, the basal areas and occupied volumes should obey mutually exclusive superposition. At the cost of extra complexity, a theory could be developed to account for this. However, the complications would not be worthwhile because (a) the basal area and occupied volume are fairly small fractions of the shelter area and volume, respectively, so the error incurred by assuming random superposition is also fairly small; (b) the error is insignificant in any case at low roughness density (more exactly, when the basal area index μ is less then about 0.1), because the difference between random and mutually exclusive superposition is then negligible.

It is clear that neither of Hypotheses I and II is an exact statement; rather, both are physically based approximations to permit a straightforward analysis. The main limitation on both is likely to occur at high roughness densities λ, where element wake interactions become so strong that there is no possibility of regarding individual wakes as separately identifiable.

3. Stress on the Ground and on the Elements

Stress on the ground

Using the above hypotheses, we consider the attenuation of ground (substrate surface) stress as roughness density increases. Suppose that n roughness elements, each with effective shelter area A, are successively placed on a large area S of the substrate surface, with the velocity U_h held constant as elements are added. When $n = 1$, (5) implies that

$$\frac{\tau_S(n=1)}{\tau_S(n=0)} = 1 - \frac{A}{S}, \tag{8}$$

where τ_S is now an average value over the large area S. (Henceforth, all stresses

are large-area averages). As more elements are added, Hypothesis II (random superposition) implies

$$\frac{\tau_S(n)}{\tau_S(0)} = \left(1 - \frac{A}{S}\right)^n \tag{9}$$

which, on introduction of the roughness density λ with (3), becomes

$$\frac{\tau_S(n)}{\tau_S(0)} = \left(1 - \frac{\lambda A}{nbh}\right)^n . \tag{10}$$

Taking the limit $n \to \infty$ with λ held constant (which means $S \to \infty$), using the well-known result $(1 + x/n)^n \to e^x$ as $n \to \infty$, and substituting for A with (7d), it follows that

$$\frac{\tau_S(\lambda)}{\tau_S(0)} = \exp\left(-\frac{\lambda A}{bh}\right) = \exp\left[-c_1\left(\frac{U_h}{u_*}\right)\lambda\right], \tag{11}$$

which shows how the stress on the ground is reduced as λ increases while U_h is held constant. A more useful expression is obtained by introducing an unobstructed drag coefficient C_S for the substrate surface, such that

$$\tau_S(\lambda = 0) = \rho C_S U_h^2 \tag{12}$$

so that (11) becomes

$$\tau_S(\lambda) = \rho C_S U_h^2 \exp\left[-c_1\left(\frac{U_h}{u_*}\right)\lambda\right] \tag{13}$$

indicating how τ_S is determined both by U_h^2 and the effect of shelter, which is described by the exponential factor.

Stress on the roughness elements

The drag force Φ on an isolated roughness element may be written as

$$\Phi = \rho C_R bh U_h^2 , \tag{14}$$

where C_R is the drag coefficient for an isolated, surface-mounted roughness element, referred to U_h as a reference wind speed. Measured values of C_R for several kinds of roughness element were collected by Taylor (1988) (who defined C_R with a factor 1/2 in (14)). These data suggest $C_R \approx 0.25$ for vertical-axis cylinders in the range of Reynolds numbers hU_h/ν between about 10^3 and 10^5, over which C_R is expected to be roughly constant by analogy with the drag coefficient for a cylinder in a free stream. For cubes, the data give $C_R \approx 0.4$ with a slight dependence on cube orientation; little Reynolds number dependence is expected in this case because of the sharp-edged nature of the obstacle.

If n elements are placed on ground area S, the force per unit ground area acting on these elements is

$$\tau_R(n) = \frac{n\Phi}{S}\left(1 - \frac{V}{Sh}\right)^n, \tag{15}$$

where Hypothesis II (random superposition of effective shelter volumes) has been invoked as in (9), with the shelter effect of each element regarded as acting entirely within the total volume of the roughness canopy envelope, Sh. Applying (3) and (14), this becomes

$$\tau_R(\lambda) = \lambda\rho C_R U_h^2\left(1 - \frac{\lambda V}{nbh^2}\right)^n \tag{16}$$

so that, substituting for V using (7d) and allowing $n \to \infty$ with λ held constant as before, we obtain

$$\tau_R(\lambda) = \lambda\rho C_R U_h^2 \exp\left(-\frac{\lambda V}{bh^2}\right) = \lambda\rho C_R U_h^2 \exp\left[-c_2\left(\frac{U_h}{u_*}\right)\lambda\right]. \tag{17}$$

This shows that τ_R increases linearly with λ in the limit $\lambda \to 0$, but as λ increases, mutual sheltering progressively attenuates τ_R.

Both τ_S and τ_R are now specified in terms of roughness geometry, by (13) and (17), respectively. Hence, both the total stress $\tau = \tau_R + \tau_S$ and the stress partition ratio τ_S/τ can be found.

4. Total Stress

From (13) and (17), the total stress is

$$\tau = \tau_S + \tau_R = \rho U_h^2\left\{C_S \exp\left[-c_1\left(\frac{U_h}{u_*}\right)\lambda\right] + \right.$$

$$\left. + \lambda C_R \exp\left[-c_2\left(\frac{U_h}{u_*}\right)\lambda\right]\right\}. \tag{18}$$

A slight complication is introduced by the appearance of the factor $U_h/u_* = ((\rho U_h)^2/\tau)^{1/2}$ in the exponents on the right-hand side, which account for sheltering of the surface and the roughness elements, respectively. Physically, this arises because roughness elements become less effective at shelter as the turbulent intensity increases, as indicated in (7). Mathematically, the consequence is that (18) is an implicit equation in τ, or more conveniently in the variable $U_h/u_* = \gamma$ (the inverse of the square root of the bulk surface drag coefficient at the roughness canopy height, $\gamma^{-1} = u_*/U_h$). To solve (18), it is helpful (though not necessary) to assume that the O(1) coefficients c_1 and c_2 are equal, say $c_1 = c_2 = c$. Loosely

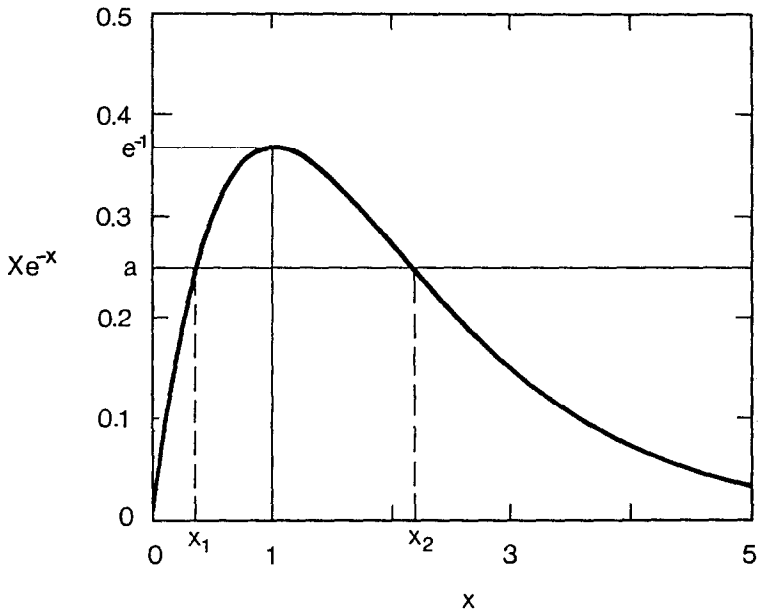

Fig. 2. The function $X\exp(-X)$, illustrating the solution of (20).

speaking, this is an assertion that elements shelter the ground and each other with the same efficiency. In fact, the solution has negligible dependence upon the ratio c_1/c_2, as discussed at the end of this section.

Setting $c_1 = c_2 = c$ and $\gamma = U_h/u_*$, (18) becomes

$$\gamma = U_h/u_* = (C_S + \lambda C_R)^{-1/2} \exp(c\lambda\gamma/2)\,, \tag{19}$$

which is an implicit equation specifying γ as a function of λ, of the form

$$Xe^{-X} = a \tag{20}$$

in the γ-like variable X, where

$$X = c\lambda\gamma/2, \quad a = (C_s + \lambda C_R)^{-1/2} c\lambda\gamma/2\,. \tag{21}$$

A sketch of the function Xe^{-X} (Figure 2) shows that (20) has the following properties:

$0 < a < e^{-1}$: two solutions, $X_1 < 1$ and $X_2 > 1$;

$a = e^{-1}$: one solution, $X = 1$;

$a > e^{-1}$: no solutions.

The correct solution from the pair X_1 and X_2 can be chosen by noting that $X \to 0$ and $a \to 0$ when $\lambda \to 0$, both from physical considerations and from (21). Since there can be only one physical solution to (20), the smaller solution X_1 is the right choice and X_2 can be discarded. It is easy to calculate X_1 iteratively; rapid

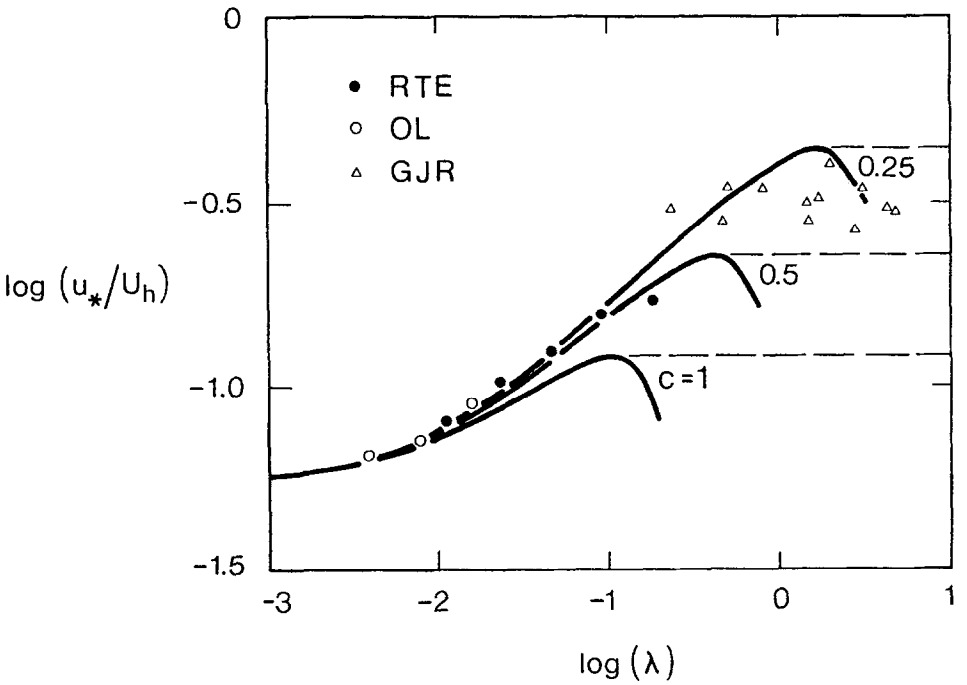

Fig. 3. Prediction of (19) (solid lines) and extrapolation (23) (dashed lines) for $\gamma^{-1} = u_*/U_h$, with $C_R = 0.30$, $C_S = 0.003$ and $c = 0.25$, 0.5 and 1.0. Points: data sets RTE, OL and GJR.

convergence is produced by writing (20) as $X_{i+1} = a \exp(X_i)$ and taking $X_0 = a$. From this solution of (20), the solution γ of the implicit Equation (19) follows immediately.

Figure 3 shows the solution of (19) as a plot of $\gamma^{-1} = u_*/U_h$ against λ, with parameters $C_R = 0.30$, $C_S = 0.0003$ and $c = 0.25$, 0.5 and 1.0. The solution has several characteristic properties. First, u_*/U_h increases with λ to a maximum value (say at $\lambda = \lambda_{max}$), decreasing thereafter. Second, u_*/U_h decreases as c increases, since c is like an extinction coefficient specifying the effectiveness of shelter in attenuating total stress. Third, the dependence of u_*/U_h on c is negligible at small λ because shelter is negligible; the corresponding solution of (19) in the limit $\lambda \to 0$ is simply $\gamma^{-1} = u_*/U_h \to (C_S + \lambda C_R)^{1/2}$, independent of c. This limiting solution is a fair approximation in practice for λ less than about 0.1. Fourth, a solution of (19) exists only when λ is less than a critical value λ_c, usually slightly higher than λ_{max}. This happens because (20) has no solution when $a > e^{-1}$; thus, from (21),

$$\lambda_c = \frac{C_R + \sqrt{C_r^2 + 4C_S(ec/2)^2}}{2(ec/2)^2} \tag{22}$$

which is the termination of each solution curve in Figure 3. A physical interpreta-

tion of the critical value λ_c does not seem possible. Instead, the nonexistence of solutions of (19) for $\lambda > \lambda_c$ is best interpreted as indicating the limitations of Hypotheses I and II at high λ values.

Also shown in Figure 3 are data on u_*/U_h from three sources:

RTE: wind tunnel data on the variation of u_*/U_h with λ for five rough surfaces with $0.011 < \lambda < 0.18$ (Raupach *et al.*, 1980). The roughness elements were vertical-axis cylinders with $h = 6$ mm and $b/h = 1$, placed on a smooth substrate. Values of U_h ranged from 12.3 to 5.8 m s^{-1}, from lowest to highest λ, while u_* ranged from 0.63 to 1.07 m s^{-1}. The roughness Reynolds number $R_h = hu_*/\nu$ was about 400, ensuring fully rough flow (which requires $R_h > 55$).

OL: wind tunnel data for three arrays of cubic elements ($b/h = 1$) on a smooth substrate (O'Loughlin, 1965). Values of λ were 1/256, 1/128 and 1/64.

GJR: low-level ($z = h$) drag coefficient data from 14 vegetation canopies and wind tunnel models of canopies, from data summaries by Garratt (1977), Jarvis *et al.* (1976) and Raupach *et al.* (1991). For these vegetated surfaces, b/h is typically less than 1, though it is difficult to specify precise values in most cases.

For the wind tunnel data sets RTE and OL, independent values of the drag coefficients C_R and C_S can be obtained. Values of C_R are about 0.25 for cylinders and 0.40 for cubes in the relevant range of hU_h/ν (Taylor 1988); the theoretical curves in Figure 3 are calculated using the single value $C_R = 0.3$. To evaluate $C_S = (u_{*S}/U_h)^2$ (where $u_{*S} = (\tau_S/\rho)^{1/2}$ is the friction velocity for the smooth substrate), one may use the law of the wall for a smooth surface, $U(z)/u_{*S} = \kappa^{-1} \ln(zu_{*S}/\nu) + B$ with $\kappa \approx 0.4$ and $B \approx 5$. The result for C_S is weakly dependent on Reynolds number and must be calculated recursively at the experimentally given value of U_h, but calculated values for both the RTE and OL data sets fall within about 20% of $C_S = 0.003$, which is the value used in Figure 3.

The solution of (19) succeeds in predicting the general behaviour of the wind tunnel data sets, RTE and OL, with $c \approx 0.5$ and thence $c_1' \approx c_2' \approx 0.5$ in (7c), since $b/h = 1$ for both data sets. Also, the single value 0.3 for C_R fits both wind tunnel data sets equally well; in fact, both sets appear to lie on the same experimental curve. There is some uncertainty about the experimental C_R values of 0.25 and 0.4 for cylinders and cubes, respectively (Taylor, 1988), and it is possible that a common value closer to 0.3 is more representative in this situation, a suggestion consistent with the near-coincidence of experimental curves of z_0/h against λ for both types of roughness elements (Koloseus and Davidian, 1966; Wooding *et al.*, 1973).

The canopy data in GJR encompass high λ values at which Hypotheses I and II are almost certainly untenable. At these roughness densities, the surface becomes "over-sheltered", so that the addition of more roughness has no further effect on u_*/U_h; instead, a progressively larger volume fraction in the lower

part of the roughness canopy is effectively stagnated, thereby removing it from interaction with the flow from the drag point of view. This implies that u_*/U_h approaches a constant value at large λ, a suggestion confirmed by the GJR data in Figure 3. It follows that a sensible extrapolation of u_*/U_h to high λ is

$$\begin{aligned} u_*/U_h &= \gamma^{-1}(\lambda) \qquad (\lambda \leqslant \lambda_{\max}), \\ u_*/U_h &= \gamma^{-1}(\lambda_{\max}) \qquad (\lambda > \lambda_{\max}), \end{aligned} \tag{23}$$

where γ is the solution of (19). The extrapolation (23) is shown by the dashed lines in Figure 3. As shown later, (23) fits the GJR canopy data well when $c \approx 0.37$.

The final point concerning total stress is the validity of the assumption $c_1 = c_2$ made after (18). An iterative solution of (18) is also possible when $c_1 \neq c_2$. This solution has been computed with c_1/c_2 varying over the wide range 0.1 to 10; it differs negligibly from the solution (19), that is, from the case $c_1 = c_2$. The physical reason for this result is that the contribution of τ_S to the total stress τ is significant only when $\lambda \ll 0.1$; in this λ range, the effect of shelter on τ_S (which is described by c_1) is insignificant. Thus, the value of c_1 is immaterial in practice for the total stress.

5. Stress Partition

The ratio of stress on the surface to total stress is given by (13) and (17):

$$\frac{\tau_S}{\tau} = \frac{C_S \exp[-c_1(U_h/u_*)\lambda]}{C_S \exp[-c_1(U_h/u_*)\lambda] + \lambda C_R \exp[-c_2(U_h/u_*)\lambda]}. \tag{24}$$

With the assumption $c_1 = c_2 = c$ made before (19), this becomes simply

$$\frac{\tau_S}{\tau} = \frac{1}{1+\beta\lambda}, \qquad \frac{\tau_R}{\tau} = \frac{\beta\lambda}{1+\beta\lambda}, \tag{25}$$

where $\beta = C_R/C_S$ is the ratio of element to surface drag coefficients. The stress partition is controlled entirely by β.

The stress partition data of Marshall (1971) (see Introduction) are compared with (25) in Figure 4, using Marshall's partition parameter $(\tau_R/\tau)^{1/2}$ as the ordinate. The prediction uses the independent drag coefficient values $C_R = 0.3$ (as in Figure 3) and $C_S = 0.0018$ (calculated for the conditions of Marshall's experiment from the law of the wall, as for Figure 3). Taking the data set as a whole, the agreement of theory with experiment is very close and is probably within the experimental scatter. Some indication of that scatter is given by the few points at high λ for which the measured value of τ_R/τ slightly exceeds 1, which is physically implausible and reflects small measurement errors. Both theory and data agree that stress partition is insignificant (in the sense that τ_R/τ is close to 1 and τ_S/τ is very small) when λ exceeds a value in the range 0.03 to 0.1. The data also show a small systematic trend with aspect ratio b/h: at given λ, τ_R/τ first decreases and

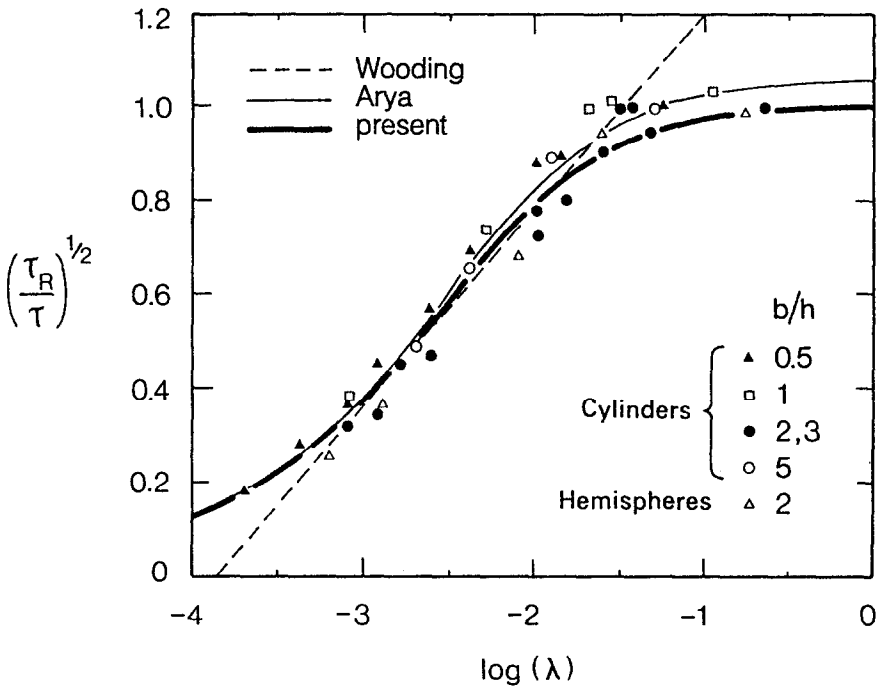

Fig. 4. Prediction (25) for stress partition, with $C_R = 0.3$ and $C_S = 0.0018$, compared with data of Marshall (1971). Ordinate is Marshall's stress partition parameter, $(\tau_R/\tau)^{1/2}$. Data are for cylinders with $b/h = 0.5$, 1, 2, 3 and 5, and hemispheres ($b/h = 2$). Also shown are predictions (25′) (Wooding *et al.*, 1973) and (25″) (Arya, 1975).

then increases again as b/h increases. This trend may reflect a dependence of the element drag coefficient C_R, and thence $\beta = C_R/C_S$, on b/h.

As in the case of total stress, one can check the sensitivity of the stress partition prediction to the assumption $c_1 = c_2$. Allowing c_1/c_2 to vary about 1 reveals a very slight, practically insignificant sensitivity of the prediction of (24) to c_1/c_2. Increasing c_1/c_2 from 1 to 3 changes τ_R/τ by only 5% at most. Decreasing c_1/c_2 from 1 to 1/3 has a negligible effect on τ_R/τ in the range $0 < \lambda < 1$, but causes difficulties when $\lambda \gg 1$ because (24) implies $\tau_R/\tau \to 0$ as $\lambda \to \infty$ if $c_1 < c_2$; this contradicts the physical requirement that $\tau_R/\tau \to 1$ as $\lambda \to \infty$. Thus, (24) yields the physical constraint $c_1 \geqslant c_2$ on c_1 and c_2, though this condition is unimportant in practice because the assumption $c_1 = c_2$ is adequate.

The stress partition prediction (25) is directly comparable with two other predictions in the literature. Wooding *et al.* (1973) suggested that

$$\left(\frac{\tau_R}{\tau}\right)^{1/2} = a_1 \ln(1/\lambda) + a_2 \qquad (25')$$

with a_1 and a_2 treated as empirical constants. This prediction is shown in Figure 4, with $a_1 = -0.18$ and $a_2 = 1.60$. It appears as a straight line which matches the

data well over a wide but limited range of λ. The limitation arises because (25′) cannot be valid in either the low-λ or the high-λ limit, since it does not satisfy the physical requirements $\tau_R/\tau \to 0$ as $\lambda \to 0$ and $\tau_R/\tau \to 1$ as $\lambda \to \infty$.

Arya (1975) developed a stress partition theory[1] for two-dimensional obstacles transverse to the mean wind, using physical hypotheses somewhat different to those made here. He obtained a prediction[2] which can be written as

$$\frac{\tau_R}{\tau} = \left[1 + \frac{(1 - a_3\lambda)}{(C_R/C_S)\lambda}\right]^{-1}, \tag{25″}$$

where a_3 (≈ 20) is an empirical constant related to the streamwise distance required for surface stress recovery downwind of an obstacle, normalized by obstacle height. This prediction is also shown in Figure 4, using the same values for C_R (0.3) and C_S (0.0018) as above. It agrees nearly as well as the present prediction (25), differing only at high λ where it predicts $\tau_R/\tau > 1$, which is physically implausible; Arya (1975) explicitly excluded this λ range from his discussion.

The main difference between the present theory and that of Arya (1975) is that (25) is free of adjustable constants, whereas (25″) is not. This occurs because the present theory assumes that obstacles shelter one another as well as the substrate surface, whereas Arya accounts for shelter of the substrate surface only. In the present theory, the effect of shelter appears through exponential drag attenuation factors with decay constants c_1 (for the substrate surface) and c_2 (for the roughness elements); taking $c_1 = c_2 = c$ leads to cancellation of all the exponential factors in (24) and the absence of adjustable constants from (25). In contrast, Arya (1975) retains a single adjustable constant equivalent to c_1. In practice, the role of the adjustable constant a_3 in the Arya prediction (25″) is weak, which corresponds to the fact that the present prediction is practically independent of c_1/c_2. As indicated before, this happens because the surface stress is significant compared with τ only at λ values $\ll 0.1$, at which sheltering is small. In other words, stress partition and inter-element sheltering are significant in different λ ranges.

6. Roughness Length

The quantity usually used in meteorology[3] to specify the drag on a rough surface is the roughness length z_0. Since z_0 is an integration constant in the inertial-sublayer velocity profile law (2), its analysis involves not only the flow within the canopy but also the flow above (in contrast with u_*/U_h and τ_R/τ, which can be

[1] The present work was carried out independently of that of Arya (1975), whose paper was pointed out to me by a referee, to whom I express my thanks.

[2] Equation (25″) corresponds to Equation (10) from Arya (1975), with allowance for his inclusion of a factor 1/2 in the definition C_R and with the substrate roughness length expressed in terms of C_S.

[3] In engineering, the "roughness function" $\Delta U/u_*$ (the increment between smooth-wall and rough-wall velocity profiles on a Clauser plot) is the more common measure. This is related to z_0 by $\Delta U/u_* = \kappa^{-1}\ln(z_0 u_*/\nu) + B$, where $\kappa \approx 0.4$ and $B \approx 5$.

analysed largely in terms of the flow within the roughness canopy). Hence, additional assumptions are needed to treat z_0. This final section is accordingly more speculative, but its inclusion is warranted because of the practical importance of z_0.

Two factors must be considered when relating z_0 to the result (23) for u_*/U_h. First, a rough surface has a finite zero-plane displacement d which must be accounted for in the profile law (2). Second, (2) is not applicable within a roughness sublayer extending above the roughness canopy to a height of order z_w. In this layer, direct dynamical effects of the canopy upon the turbulence are apparent; the main effect in the present context is to make the eddy diffusivity for momentum greater than the inertial-sublayer diffusivity $\kappa u_*(z-d)$, by a factor of up to 2 at $z=h$ (Garratt, 1980; Raupach *et al.*, 1980; Raupach *et al.*, 1991).

Accounting for both complications, a profile law valid both above and within the roughness sublayer ($h < z < z_w$) may be written as

$$\frac{\kappa U(z)}{u_*} = \ln\left(\frac{z-d}{z_0}\right) + \Psi\left(\frac{z-d}{z_w-d}\right), \tag{26a}$$

where Ψ is a profile influence function accounting for the departure of the actual momentum diffusivity within the roughness sublayer from $\kappa u_*(z-d)$, equivalent to the well-known stability influence function which accounts for diabatic effects on the profile shape. In particular,

$$U_h/u_* = \gamma = \frac{1}{\kappa}\left[\ln\left(\frac{h-d}{z_0}\right) + \Psi_h\right], \tag{26b}$$

where Ψ_h is the value of Ψ at $z=h$. Hence

$$\frac{z_0}{h} = \frac{h-d}{h}\exp(\Psi_h)\exp(-\kappa\gamma) \tag{27}$$

which is the basic relationship between z_0/h and γ. It involves both Ψ_h and d/h.

The profile influence function Ψ

An approximate form for Ψ can be derived using the observation that velocity profiles within the roughness sublayer (after spatial averaging to account for element-scale heterogeneity) are quite well described by taking the eddy diffusivity to be constant at $\kappa u_*(z_w-d)$. This gives a velocity profile for $h < z < z_w$

$$\frac{\kappa(U(z)-U(z_w))}{u_*} = \frac{z-z_w}{z_w-d} \tag{28}$$

which is experimentally verified by Raupach *et al.* (1980). Hence, by subtracting (2) from (28), a form is obtained for Ψ:

$$\Psi\left(\frac{z-d}{z_w-d}\right) = \ln\left(\frac{z_w-d}{z-d}\right) + \frac{z_w-z}{z_w-d}. \tag{29}$$

It is now necessary to know z_w. Two external governing length scales for z_w have been suggested previously: the inter-element separation D (Garratt, 1980) and the element breadth b (Raupach *et al.*, 1980). Both of these suggestions lead to complicated forms for Ψ which, when used in (27), fail to describe the data set for z_0/h shown later in Figure 5c (it is not necessary to go through the analytical details). A more successful expression for Ψ can be derived from the proposal that the distinctive dynamics of the flow near $z = h$ arise from the intense shear layer centred near $z = h$ and induced by the drag of the canopy on fluid below $z = h$ (Raupach *et al.*, 1989). This causes the turbulent flow near $z = h$ to resemble the flow in a free shear layer rather than turbulent boundary layer, and therefore to have an eddy diffusivity for momentum which is determined by the vertical length scale of the layer of intense shear, $h - d$. It follows that

$$z_w - d = c_w(h - d)\,, \tag{30}$$

where c_w is a constant greater than 1 (to ensure $z_w > h$). Substitution of (30) into (29) gives

$$\Psi_h = \ln(c_w) + 1 - c_w^{-1} \tag{31}$$

which is a simple result independent of all surface length scale ratios (in contrast with the result obtained by assuming that z_w scales with D or b). From velocity profile data in the roughness sublayer (O'Loughlin, 1965; Raupach *et al.*, 1980), c_w can be estimated to be 1.4 to 1.8, implying $\Psi_h \approx 0.62$ to 1.03. The value adopted here is $c_w = 1.5$, giving $\Psi_h = 0.74$.

The zero-plane displacement d

Thom (1971) proposed that d is the mean level of momentum absorption by a rough surface or the centroid of the drag force profile, a suggestion supported theoretically by Jackson (1981). Here, d is estimated from scaling arguments similar to those used to estimate the effective shelter area A and volume V. It is proposed that the centroid of the drag force profile is governed by the vertical spread of the strong shear layer formed behind a typical roughness element, and in particular by the vertical distance over which the shear layer can spread before it reaches the next element downwind. This implies that $(h - d_R)/D \sim u_*/U_h = \gamma^{-1}$, where D is a typical streamwise inter-element distance and d_R is the centroid of the drag force τ_R (per unit area) acting on the roughness elements only. Since $\lambda \sim bh/D^2$, it follows that

$$(h - d_R)/h = c_d(b/(h\lambda))^{1/2}\gamma^{-1}\,, \tag{32}$$

where c_d is an O(1) constant. Accounting for the drag on the ground, the overall centroid of the drag force profile is $d = (\tau_R d_R + \tau_S d_S)/\tau = (\tau_R/\tau)d_R$, because the

centroid d_S of the drag on the substrate surface is zero. Hence, using (25), the result for d is

$$\frac{d}{h} = \frac{\tau_R}{\tau}\left(1 - c_d\left(\frac{b}{h\lambda}\right)^{1/2}\gamma^{-1}\right)$$

$$= \left(\frac{\beta\lambda}{1+\beta\lambda}\right)\left(1 - c_d\left(\frac{b}{h\lambda}\right)^{1/2}\gamma^{-1}\right) \tag{33}$$

with the constraint $d/h \geqslant 0$. Best agreement with data is obtained when $c_d \approx 0.6$.

Comparisons with observations

Figure 5 shows the predictions (23) for u_*/U_h, (33) for d/h and (27), with (31) and (33), for z_0/h. Available data from the sets RTE, OL and GJR are also shown. The drag coefficient values are the same as in Figure 3. The constant c in (19) has been set at 0.37, so that u_*/U_h is correctly predicted for the canopy (GJR) data at $\lambda > \lambda_{\max}$, where $u_*/U_h \approx 0.3$.

The other two constants which must be set are c_w in (31) and c_d in (33). The effect of varying c_w is simply to multiply z_0/h by the factor $\exp(\Psi_h) = c_w \exp(1 - c_w^{-1})$. This factor, and hence c_w, are closely constrained by the z_0/h data at low λ, where the prediction for z_0/h is nearly independent of both c and d/h. This constraint requires $c_w = 1.5 \pm 0.1$, which is consistent with independent evidence that c_w is between 1.4 and 1.8 (see above). Finally, the value of c_d is set at 0.6 to give best agreement with data. The predictions for $c_d =$ 0.3, 0.6 and 1.2 are shown in Figure 5.

7. Discussion and Conclusions

For a surface covered in roughness elements, theoretical predictions have been developed to describe (a) the total stress (specifically the square root of the drag coefficient, $\gamma^{-1} = u_*/U_h$); (b) the stress partition (specifically the ratios τ_R/τ and τ_S/τ, where τ_R, τ_S and $\tau = \tau_R + \tau_S$ are the stresses on the substrate, the roughness elements and the entire rough surface, respectively); (c) the zero-plane displacement d; and (d) the roughness length z_0.

The theory for $\gamma^{-1} = u_*/U_h$ and τ_R/τ is based on the idea that the wake and drag properties of an isolated roughness element can be characterized by an effective shelter area A and shelter volume V, which respectively describe the surface stress deficit behind the element and the attenuation of drag on other obstacles in the element wake. Two hypotheses (I and II) are introduced: I to scale A and V in terms of element dimensions and flow properties, and II to specify how the wakes of different elements interact. Both hypotheses are physically based at low roughness density λ, but are unlikely to hold at high λ. This is apparent in the solution for $\gamma^{-1} = u_*/U_h$, which exists only for $\lambda < \lambda_c$ where the critical value

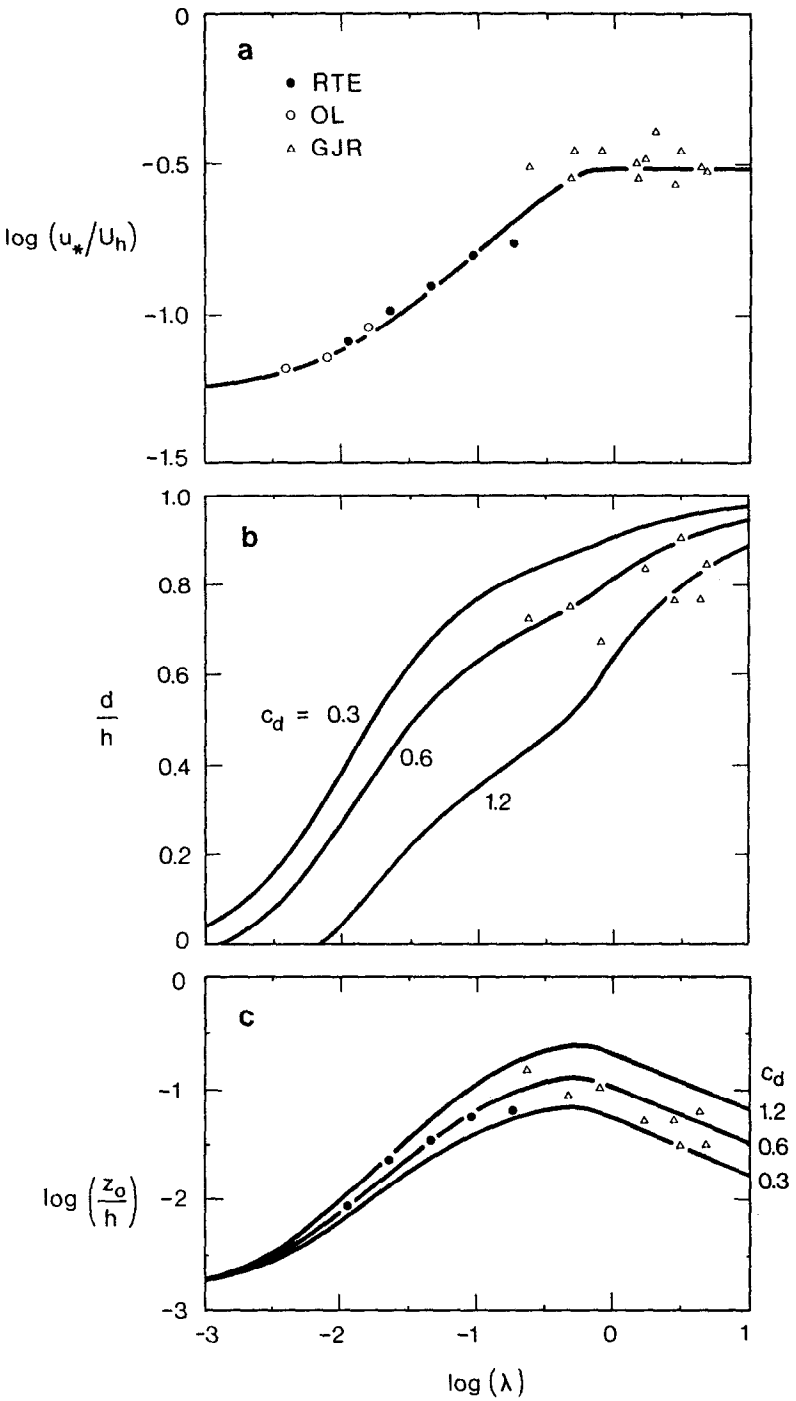

Fig. 5. Predicted dependence upon λ of (a) u_*/U_h, from (23); (b) d/h, from (33); (c) z_0/h, from (27) and (31). Constants: $C_R = 0.3$, $C_S = 0.003$, $c = 0.37$, $c_w = 0.5$, $c_d = 0.3$, 0.6 and 1.2. Data as in Figure 3.

λ_c is typically of order 1. To circumvent this, it is appropriate to replace the solution from Hypotheses I and II at high λ with a constant $\gamma^{-1} = u_*/U_h$.

The stress partition prediction is the very simple equation $\tau_R/\tau = \beta\lambda/(1 + \beta\lambda)$, where $\beta = C_R/C_S$ is the ratio of element and surface drag coefficients. This prediction agrees very well with data (Figure 4) and is free of adjustable constants. It implies that, for typical rough surfaces, stress partition is insignificant (in the sense that τ_S/τ is very small) when λ exceeds a value in the range 0.03 to 0.1.

The prediction for total stress is the solution of the implicit Equation (19), modified at high λ to give constant u_*/U_h as in (23). The prediction includes a pair of constants c_1 and c_2 introduced by Hypothesis I, which determine the effectiveness with which the elements shelter the surface and one another, respectively. The value of c_1 and the ratio c_1/c_2 are immaterial in practice, because the substrate surface stress only contributes to the total stress in a λ range ($\lambda \ll 0.1$) where the surface shelter described by c_1 is insignificant. Therefore, one can take $c_1 = c_2 = c$, a single constant, to obtain mathematical simplification. The value of c is roughly 0.5 for roughness elements with aspect ratios b/h close to 1, but is not well determined by the available data. Aspect ratio influences c because $c = c_{1,2} = c'_{1,2}(b/h)^p$, where c'_1 and c'_2 are O(1) constants, and the power p is 1 for $h \gg b$ and 0 for $b \gg h$ (see (7c) and (7d)).

As $\lambda \to 0$, inter-element sheltering becomes negligible and the prediction for total stress becomes independent of c: $u_*/U_h \to (C_s + \lambda C_R)^{1/2}$. In practice this approximation is reasonable for λ less than about 0.1, so for much of the λ range of interest for sparse roughness (and most of the range over which Hypotheses I and II are applicable), uncertainty about c is not important. Inter-element sheltering is important only when λ exceeds 0.1, in contrast with stress partition which is important only when λ is less than 0.1.

For the total stress prediction to fit vegetation canopy data at high λ, where $u_*/U_h \approx 0.3$ and is approximately independent of λ, it is necessary that $c = 0.37$. However, c can no longer be interpreted at high λ in the same way as at low λ, because of the inapplicability of Hypotheses I and II.

The theory for d/h and z_0/h requires additional physical considerations and hypotheses, to describe d/h as the centre of action of the drag force within the roughness and to account for the roughness sublayer above the canopy. Two O(1) constants are thereby introduced in addition to c: c_w in (31) and c_d in (33). Both are tightly constrained. Data on d/h and z_0/h are predicted satisfactorily only if $c_w \approx 1.5$ and $c_d \approx 0.6$.

References

Arya, S. P. S.: 1975, 'A Drag Partition Theory for Determining the Large-Scale Roughness Parameter and Wind Stress on the Arctic Pack Ice', *J. Geophys. Res.* **80**, 3447–3454.

Bandyopadhyay, P. R.: 1987, 'Rough-Wall Turbulent Boundary Layers in the Transition Regime', *J. Fluid Mech.* **180**, 231–266.

Batchelor, G. K.: 1967, *An Introduction to Fluid Dynamics*, Cambridge University Press, Cambridge, 615 pp.

Finnigan, J. J., Raupach, M. R., Bradley, E. F., and Aldis, G. K.: 1990, 'A Wind Tunnel Study of Turbulent Flow over a Two-Dimensional Ridge', *Boundary-Layer Meteorol.* **50**, 277–317.

Garratt, J. R.: 1977, 'Aerodynamic Roughness and Mean Monthly Surface Stress over Australia', *Div. Atmos. Phys. Tech.* Pap. 29, CSIRO, Australia.

Garratt, J. R.: 1980, 'Surface Influence upon Vertical Profiles in the Atmospheric Near Surface Layer', *Quart. J. Roy. Meteorol. Soc.* **106**, 803–819.

Jackson, P. S.: 1981, 'On the Displacement Height in the Logarithmic Velocity Profile', *J. Fluid Mech.* **111**, 15–25.

Jarvis, P. G., James, G. B., and Landsberg, J. J.: 1976, 'Coniferous Forest', in J. L. Monteith (ed.), *Vegetation and the Atmosphere*, Vol. 2, Academic Press, London, p. 171–240.

Koloseus, H. J. and Davidian, J.: 1986, 'Free-surface Instability Correlations, and Roughness-Concentration Effects on Flow over Hydrodynamically-Rough Surfaces', *USGS Water Supply Pap. 1592 C.*

Lettau, H.: 1969, 'Note on Aerodynamic Roughness-Parameter Estimation on the Basis of Roughness-Element Description', *J. Appl. Meteorol.* **8**, 828–832.

Lighthill, J.: 1986, *An Informal Introduction to Theoretical Fluid Mechanics*, Clarendon Press, Oxford, 260 pp.

Marshall, J. K.: 1971, 'Drag Measurements in Roughness Arrays of Varying Density and Distribution', *Agric. Meteorol.* **8**, 269–292.

O'Loughlin, E. M.: 1965, 'Resistance to Flow over Boundaries with Small Roughness Concentrations', Ph.D. Dissertation, University of Iowa.

Raupach, M. R., Antonia, R. A. and Rajagopalan, S.: 1991, 'Rough-Wall Turbulent Boundary Layers', *Appl. Mechs. Revs.* **44**, 1–25.

Raupach, M. R., Finnigan, J. J., and Brunet, Y.: 1989, 'Coherent Eddies in Vegetation Canopies', *Proc. Fourth Australasian Conf. on Heat and Mass Transfer*, Christchurch, New Zealand, 9–12 May, 1989, pp. 75–90.

Raupach, M. R., Gillette, D. A., and Leys, J. F.: 1992, 'The Effect of Roughness Elements on Wind Erosion Threshold', *J. Geophys. Res.* (submitted).

Raupach, M. R., Thom, A. S. and Edwards, I.: 1980, 'A Wind Tunnel Study of Turbulent Flow Close to Regularly Arrayed Rough Surfaces', *Boundary-Layer Meteorol.* **18**, 373–397.

Schlichting, H.: 1936, 'Experimentelle Untersuchungen zum Rauhigkeitsproblem', *Ing.-Arch.* **7**, 1–34; *NACA Tech. Mem.* 823.

Shaw, R. H. and Pereira, A. R.: 1982, 'Aerodynamic Roughness of a Plant Canopy: a Numerical Experiment', *Agric. Meteorol.* **26**, 51–65.

Taylor, P. A.: 1988, 'Turbulent Wakes in the Atmospheric Boundary Layer', in W. L. Steffen and O. T. Denmead (eds.), *Flow and Transport in the Natural Environment: Advances and Applications*, Springer-Verlag, Berlin, p. 270–292.

Thom, A. S.: 1971, 'Momentum Absorption by Vegetation', *Quart. J. Roy. Meteorol. Soc.* **97**, 414–428.

Wooding, R. A., Bradley, E. F., and Marshall, J. K.: 1973, 'Drag Due to Regular Arrays of Roughness Elements of Varying Geometry', *Boundary-Layer Meteorol.* **5**, 285–308.

Yaglom, A. M.: 1979, 'Similarity Laws for Constant-Pressure and Pressure-Gradient Turbulent Wall Flows', *Ann. Rev. Fluid Mech.* **11**, 505–540.